Brief communication: An elliptical parameterisation of the wind direction rose

Edward Hart[1]

[1]Wind Energy and Control Centre, Department of Electronic and Electrical Engineering, University of Strathclyde, Glasgow, United Kingdom

Correspondence: Edward Hart (edward.hart@strath.ac.uk)

Abstract. This brief communication presents a parametric model for the wind direction rose, based on ellipse geometry. Such a model supports standardisation and identification of generally representative cases, while also enabling systematic analyses of wind rose "shape" impacts on the benefits of proposed wind farm design and control innovations. Formulations include analytical wind direction rose modelling, model fitting to measured data via gradient descent minimisation of sum-of-square-
5 errors, and goodness-of-fit measures. Testing on wind direction data from real offshore wind farms confirms good performance, indicating this parametric model is useful to wind energy research and development efforts.

1 Introduction

At the wind farm scale, the direction of the wind strongly affects the levels of turbine-turbine interactions and, hence, the flow conditions experienced by individual turbines (Meyers et al., 2022; Dallas et al., 2023). This, in turn, impacts energy
10 production, optimal turbine layout, the efficacy of different wind farm control strategies, and turbine reliability (Slot et al., 2018; Amiri et al., 2019; King et al., 2021; Stanley et al., 2023). The wind direction rose is therefore of broad importance to wind farm design and operation. Despite this, to the best of the authors knowledge, a standard parametric model for the wind direction rose is yet to be adopted by the industry. The benefits of such a model would include: 1) allowing for standardisation and supporting the identification of typical or generally representative cases[1] 2) enabling the impacts of wind rose "shape" on
15 the energy yield and reliability resulting from proposed innovations to be systematically explored. For example, recent studies on wake steering and turbine layout optimisation (King et al., 2021; Stanley et al., 2023) report the energy uplift obtained for a single candidate wind rose. The robustness and generality of these studies would be enhanced if, instead, energy uplift were determined across a range of wind roses, obtained by systematically varying model parameters. While direction inclusive joint probability distributions have been proposed in the literature, their complexity and large parameter-sets render them impractical
20 for such applications (Yang et al., 2022; Yang and Dong, 2024). This brief communication therefore proposes a novel simple parametric model for the wind direction rose, utilising ellipse geometry to minimise the number of parameters required.

---

[1]For example, we see this for wind speed distributions, where a Weibull distribution with shape parameter close to 2 is common (Shu and Jesson, 2021).

Section 2 develops the parametric wind direction rose model, along with necessary theory to allow for fitting to measured data and evaluation of goodness-of-fit. Example implementations are then provided in Section 3, before Section 4 concludes the paper.

2 Methodology

2.1 Standard ellipse equations

The ellipse, which generalises the concept of a circle, has the following standard parametric form,

$$(x,y) = (a\cos(\theta), b\sin(\theta)) \ \text{ for } 0 \leq \theta \leq 2\pi,$$

where the ellipse's axes (of length $2a$ and $2b$) align with the coordinate system's x and y axes, respectively. More generally, if the ellipse is rotated by an angle ϕ while remaining centered at the origin, its parametric form becomes,

$$
\begin{aligned}
(x,y) \quad = \quad \big(\, &a\cos(\theta)\cos(\phi) - b\sin(\theta)\sin(\phi), \\
&a\cos(\theta)\sin(\phi) + b\sin(\theta)\cos(\phi)\big) \\
&\text{for } 0 \leq \theta \leq 2\pi,
\end{aligned}
$$

Note, any ellipse of the latter form may be reduced to the former via a simple change of coordinates. Without loss of generality we therefore focus on the first parametric form.

It is further assumed, again without loss of generality, that $a > b$. In this case, a is called the semi-major axis and b is called the semi-minor axis. This being the case, the "shape" of the ellipse may be captured via its eccentricity,

$$e = \sqrt{1 - \frac{b^2}{a^2}}.$$

Eccentricity, which falls between 0 and 1, may be interpreted as a dimensionless measure of the ellipse's "deviation" from being circular. When $e = 0$ the ellipse is circular, with the ellipse becoming increasingly long and flat as $e \to 1$. The total area enclosed by an ellipse is,

$$A = \pi a b.$$

2.2 Ellipses of unit area

Imposing the restriction $A = 1$ it follows that,

$$b = \frac{1}{\pi a},$$

and, hence, the number of parameters defining the ellipse is reduced to one, i.e. just a. A one-to-one correspondence between a and e then exists in this restricted case,

$$e \quad = \quad \sqrt{1 - \frac{1}{\pi^2 a^4}}.$$
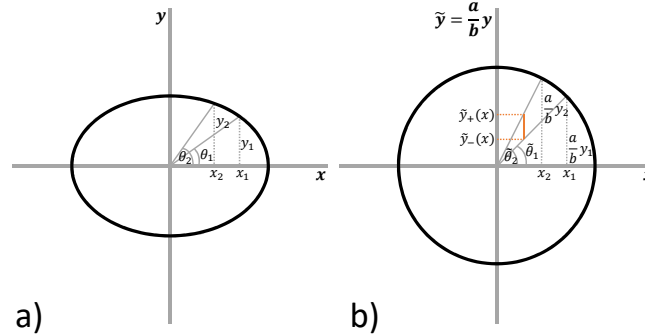
Figure 1. Ellipse (a) and scaled-ellipse (b) geometry.

Recall that this specific formula holds for $a > b$, which in this case is when $a > 1/\pi a$. An ellipse of unit area may be naturally

50 interpreted as a wind direction rose by defining the probability of the wind blowing from between directions θ_1 and θ_2 to be equal to the area enclosed by the ellipse between those two angles. As such, a formula for ellipse segment areas is required. This may be obtained by observing that an ellipse with semi-major axis a (aligned with x) and semi-minor axis b (aligned with y) becomes a circle if the y-axis is scaled by a factor of a/b (see Figure 1). This scaling effects the segment angles θ_1 and θ_2, resulting in adusted angles (for a unit-area-ellipse) of,

$$
55 \quad \tilde{\theta}_1 \;=\; \tan^{-1}\left(\frac{a}{b} \cdot \frac{y_1}{x_1}\right) = \tan^{-1}\left(\pi a^2 \tan(\theta_1)\right)
$$

$$
\tilde{\theta}_2 \;=\; \tan^{-1}\left(\frac{a}{b} \cdot \frac{y_2}{x_2}\right) = \tan^{-1}\left(\pi a^2 \tan(\theta_2)\right).
$$

The area of the circle segment in scaled axes is simply,

$$
\pi a^2 \left(\frac{\tilde{\theta}_2 - \tilde{\theta}_1}{2\pi}\right) = \frac{1}{2}a^2\left(\tilde{\theta}_2 - \tilde{\theta}_1\right). \tag{1}
$$

Observing that segment areas may, in general, be written in the form (see Figure 1),

$$
60 \quad \int_0^{x_1} \left(\tilde{y}_+(x) - \tilde{y}_-(x)\right) dx,
$$

it readily follows that scaling the y-axis directly scales the calculated area. As such, the area bounded by θ_1 and θ_2 within the unit-area-ellipse (in the original coordinate system) is given by,

$$
\begin{aligned}
A_{\theta_1,\theta_2} \;=\;& \frac{b}{a} \cdot \frac{1}{2}a^2\left(\tilde{\theta}_2 - \tilde{\theta}_1\right) \\
\;=\;& \frac{1}{2\pi}\Bigg(\tan^{-1}\left(\pi a^2 \tan(\theta_2)\right) \\
& - \tan^{-1}\left(\pi a^2 \tan(\theta_1)\right) \Bigg).
\end{aligned} \tag{2}
$$

2.3 An elliptical wind direction rose

As outlined above, an ellipse of unit area may be naturally interpreted as a wind direction rose, with the probability associated with each direction segment equal to its area - all of which is determined by the single parameter, a. Consider the case where wind directions bins are centered on values $\theta_{c,i}$ (including 0 and $\pi/2$ rads) and of width $2\delta\theta$, where $i = 1,\ldots,2\pi/2\delta\theta$. The

70 *elliptical wind direction rose* with elliptical parameter a is defined as,

$$P_{\text{el}}(\theta_{\text{wind}} = \theta_{c,i}, a) = \begin{cases} A_{\theta_{c,i+},\theta_{c,i-}} & \text{if } \theta_{c,i} > 0 \text{ and } \theta_{c,i} < \pi/2 \\ 2A_{\delta\theta,0} & \text{if } \theta_{c,i} = 0 \\ 2A_{\frac{\pi}{2},\frac{\pi}{2}-\delta\theta} & \text{if } \theta_{c,i} = \pi/2 \\ \text{Obtained via symmetries} & \\ \text{if } \pi/2 < \theta_{c,i} < 2\pi, \end{cases}$$

where $\theta_{c,i+} = \theta_{c,i} + \delta\theta$ and $\theta_{c,i-} = \theta_{c,i} - \delta\theta$. Note also that $\tan^{-1}\left(\pi a^2 \tan(\pi/2)\right) = \pi/2$. As indicated above, directional probabilities outside the first quadrant may be obtained via symmetries, by reflecting those values across horizontal and/or vertical axes. In computational terms, this amounts to copying, reordering and concatenating the relevant numerical arrays. As

75 a result of these same symmetries, it follows that bins which are opposite (in the context of reflections about the vertical axis) have identical probabilities, i.e.,

$$P_{\text{el}}(\theta_{\text{wind}} = \theta_{c,i}, a) = \begin{cases} P_{\text{el}}(\theta_{\text{wind}} = \pi - \theta_{c,i}, a) \\ \text{if } \theta_{c,i} > 0 \text{ and } \theta_{c,i} < \pi/2, \\ P_{\text{el}}(\theta_{\text{wind}} = 3\pi - \theta_{c,i}, a) \\ \text{if } \theta_{c,i} > \frac{3\pi}{2} \text{ and } \theta_{c,i} < 2\pi. \end{cases}$$

The latter case was written in the above form to maintain all angles between 0 and 2π. Symmetrical "circular" and "bi-directional" wind roses may therefore be readily obtained by setting only a single parameter, a. Via rotation of the resulting

80 elliptical wind rose, one may then set the principal direction in bi-directional cases.

2.4 Specifying a prevailing wind direction - the folding parameter

Many sites are not be equally bi-directional, and instead have a single prevailing wind direction which dominates. To account for such cases, one may take an elliptical (non-rotated) wind rose and reallocate (i.e,"fold") a certain proportion of probability mass from left-hand-plane segments onto their right-half-plane counterparts. This results in a wind rose with a single prevailing

85 wind direction. Formally, the *generalised elliptical wind direction rose* with elliptical parameter a and folding parameter f

$(0 \leq f \leq 1)$ is defined as,

$$
P_{\mathrm{g}}(\theta_{\mathrm{wind}} = \theta_{c,i}, a, f) =
\begin{cases}
(1-f)P_{\mathrm{el}}(\theta_{\mathrm{wind}} = \theta_{c,i}, a) \\[4pt]
\quad \text{if } \pi/2 < \theta_{c,i} < 3\pi/2, \\[8pt]
(1+f)P_{\mathrm{el}}(\theta_{\mathrm{wind}} = \theta_{c,i}, a) \\[4pt]
\quad \text{if } 0 \leq \theta_{c,i} < \pi/2 \text{ or } 3\pi/2 < \theta_{c,i} \leq 2\pi, \\[8pt]
P_{\mathrm{el}}(\theta_{\mathrm{wind}} = \theta_{c,i}, a), \\[4pt]
\quad \text{if } \theta_{c,i} = \pi/2 \text{ or } 3\pi/2.
\end{cases}
$$

The symmetries in the elliptical distribution of directional probabilities guarantee this generalised parametric form is a true probability distributions, i.e. the sum of all directional probabilities remains 1.

90   As previously, this generalised wind direction rose may be rotated in order to specify a prevailing wind direction, θ_{prev}. Formally,

$$
P_{\mathrm{g}}^{\dagger}(\theta_{\mathrm{wind}} = \theta_{c,i}, a, f, \theta_{\mathrm{prev}}) = P_{\mathrm{g}}(\theta_{\mathrm{wind}} = \theta_{c,i} - \theta_{\mathrm{prev}}, a, f).
$$

2.5   Fitting a generalised elliptical wind direction rose to measured data

Assume we have a vector of wind direction-segment probabilities, $\widehat{\mathbf{P}}$, obtained from measured data and specified for a given

95   set of wind direction bins, centered on values $\boldsymbol{\theta}_c$ (each of width $2\delta\theta$). Further, we assume the circular mean (Dallas et al., 2023) of the measured wind direction data is known. The prevailing wind direction, θ_{prev}, of the parametric model is set equal to the bin centre-value, denoted $\bar{\theta}_{\mathrm{c}}$, of the bin into which the directional mean falls. Alternatively, θ_{prev} may be set equal to the centre-angle of the direction bin with largest probability mass (the mode direction). The best approach in practice was found to be that of fitting both cases, then keeping the one which results in the smallest error. Fitting a generalised elliptical wind

100   direction rose to $\widehat{\mathbf{P}}$ may then be formulated in the context of sum-of-square-errors,

$$
\mathrm{SSE}(a, f) = \sum_{i=1}^{2\pi/2\delta\theta} \left(P_{\mathrm{g}}^{\dagger}(\theta_{\mathrm{wind}} = \theta_{c,i}, a, f, \theta_{\mathrm{prev}}) - \widehat{P_i} \right)^2,
$$

specifically, the minimisation thereof with respect to parameters a and f,

$$
\min_{a, f} \; \mathrm{SSE}(a, f).
$$

Since $a > 0$ and $0 \leq f \leq 1$, a constrained optimisation would be required for the problem in its current form. However, observ-

105   ing that only a^2 appears within the fitting formulation (Equation 2), the constraint on a may simply be removed for the purposes of optimisation, and then reinstated by taking the absolute value of the result. Unconstrained optimisation which respects the restriction on f may be achieved by setting,

$$
f = \frac{1}{1 + e^{-\phi_f}}
$$

and performing unconstrained optimisation over ϕ_f. Partial derivatives may then be obtained, allowing for gradient-descent
based optimisation:

$$
\frac{\partial \mathrm{SSE}}{\partial a}(a, f) = \sum_{i=1}^{2\pi/2\delta\theta} 2\left(P_{\mathrm{g}}^{\dagger} - \widehat{P}_i\right)\frac{\partial P_{\mathrm{g}}^{\dagger}}{\partial a}
$$

$$
\frac{\partial \mathrm{SSE}}{\partial \phi_f}(a, f) = \sum_{i=1}^{2\pi/2\delta\theta} 2\left(P_{\mathrm{g}}^{\dagger} - \widehat{P}_i\right)\frac{\partial P_{\mathrm{g}}^{\dagger}}{\partial \phi_f}
$$

$$
\frac{\partial A_{\theta_1, \theta_2}}{\partial a} = \frac{a\tan(\theta_2)}{\pi^2\tan^2(\theta_2)a^4 + 1} - \frac{a\tan(\theta_1)}{\pi^2\tan^2(\theta_1)a^4 + 1}
$$

$$
\frac{\partial P_{\mathrm{g}}^{\dagger}}{\partial \phi_f} = \begin{cases} -f^2 e^{-\phi_f}\, P_{\mathrm{el}}(\theta_{\mathrm{wind}} = \tilde{\theta}_{c,i}, a) \\[4pt] \text{if } \pi/2 < \tilde{\theta}_{c,i} < 3\pi/2, \\[8pt] f^2 e^{-\phi_f}\, P_{\mathrm{el}}(\theta_{\mathrm{wind}} = \tilde{\theta}_{c,i}, a) \\[4pt] \text{if } 0 \leq \tilde{\theta}_{c,i} < \pi/2 \text{ or } 3\pi/2 < \tilde{\theta}_{c,i} \leq 2\pi, \\[8pt] 0, \\[4pt] \text{if } \tilde{\theta}_{c,i} = \pi/2 \text{ or } 3\pi/2. \end{cases}
$$

where $\tilde{\theta}_{c,i} = \theta_{c,i} - \theta_{\mathrm{prev}}$. The partial derivative $\partial P_{\mathrm{g}}^{\dagger}/\partial a$ is readily obtained using $\partial A_{\theta_1, \theta_2}/\partial a$, however, the full expression is
not included for the sake of brevity.

2.5.1 Assessing goodness-of-fit

A coefficient of determination, typically denoted R^2, may be calculated for the resulting fit to measured data:

$$
R^2 = 1 - \frac{\sum_{i=1}^{2\pi/2\delta\theta}\left(P_{\mathrm{g}}^{\dagger}(\theta_{\mathrm{wind}} = \theta_{c,i}, a, f, \theta_{\mathrm{prev}}) - \widehat{P}_i\right)^2}{\sum_{i=1}^{2\pi/2\delta\theta}\left(\widehat{P}_i - \overline{\widehat{\mathbf{P}}}\right)^2},
$$

with $\overline{\widehat{\mathbf{P}}}$ the mean of all measured directional probabilities. This value falls between 0 and 1 and describes the proportion of
total variance, present in the measured data, captured by the fitted model. The root-mean-squared-error may also be calculated
when assessing goodness of fit,

$$
\mathrm{RMSE} = \sqrt{\frac{2\delta\theta}{2\pi}\sum_{i=1}^{2\pi/2\delta\theta}\left(P_{\mathrm{g}}^{\dagger}(\theta_{\mathrm{wind}} = \theta_{c,i}, a, f, \theta_{\mathrm{prev}}) - \widehat{P}_i\right)^2}.
$$

3 Results

Example generalised elliptical wind direction roses are shown in Figure 2, along with their associated parameter values. This
demonstrates the flexibility of the proposed parametric model. Each direction rose may be rotated to obtain any required
prevailing wind direction (or directions, when $f = 0$).
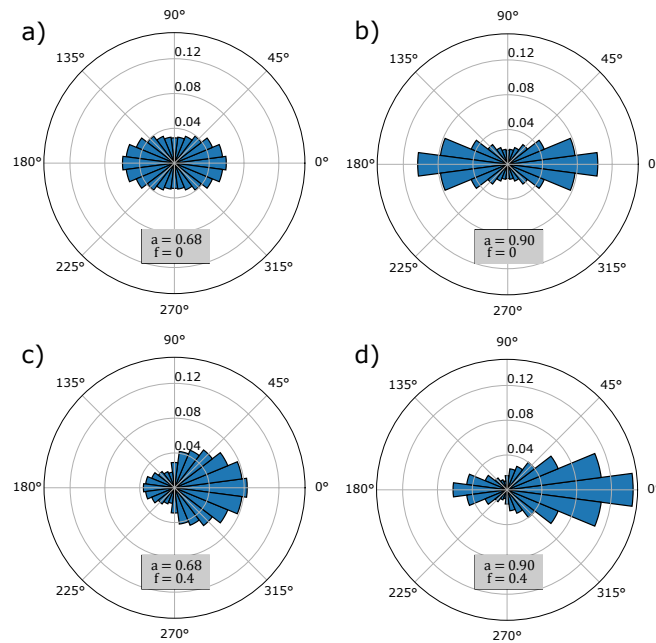
Figure 2. Example generalised elliptical wind direction roses, showcasing the various forms the parametric model can generate. Parameter values are given in each case.

Results from fitting the parametric model to real wind direction rose data are shown in Figure 3. A good fit is achieved in most cases, indicating the proposed model is representative of real wind direction roses. Goodness-of-fit values highlight the

130 fact that the RMSE-scale is dependent on the number of wind direction bins. Since R^2 values are normalised, they can be seen to provide a strong indication of model fit-quality that is independent of the number of bins. Limitations of R^2 should be kept in mind when utilising it to assess goodness-of-fit (Hahn, 1973; Barrett, 1974). However, in the current case the aim is not that of producing a predictive model, hence, the main limitations of R^2 are unlikely to be of significance here. It is interesting to note that the various fitted parametric models include both mean and mode θ_{prev} cases, as well as cases where the two coincide.

135 Finally, results highlight that a good fit to measured data will not be achieved in all cases (Figure 3e), but, such instances will be flagged by low R^2 scores.

4 Conclusions

A parametric model for the wind direction rose has been presented, based on ellipse geometry and extended to allow specification of a prevailing wind direction. Relevant equations were developed to allow the parametric model to be fitted to measured

140 data, via gradient descent minimisation of sum-of-square-errors. Testing on real offshore wind farm data indicated the parametric model is indeed representative. R^2 and RMSE goodness-of-fit measures were utilised, with the former providing a strong indication of model suitability which is independent of the number of direction bins. It was highlighted that the proposed para-
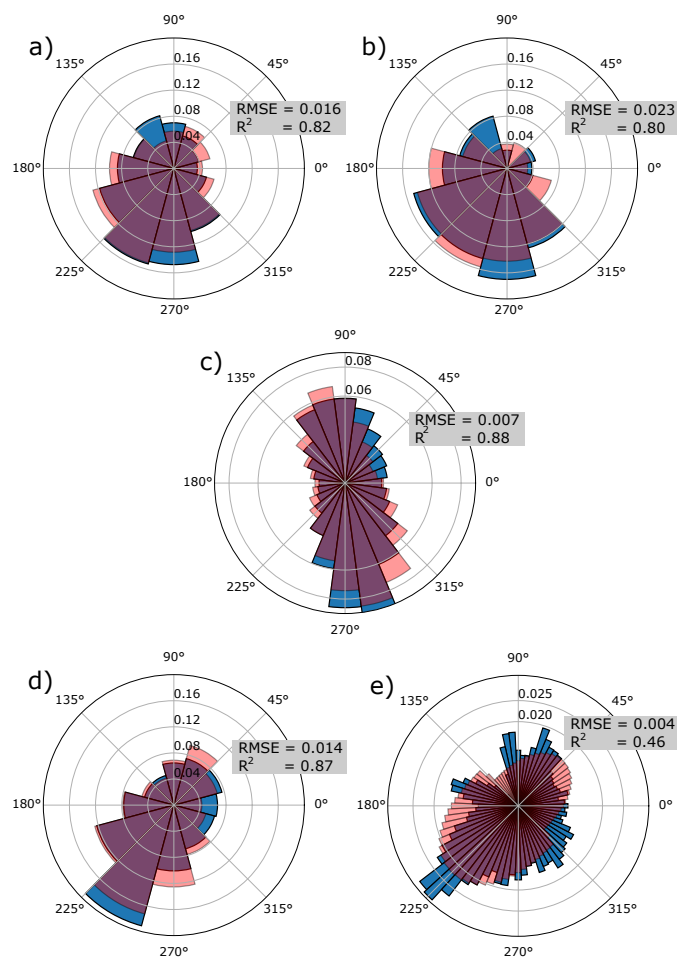
Figure 3. Wind direction roses as measured at real offshore wind farms (blue), and the corresponding best-fit generalised elliptical wind direction model (red) in each case. Goodness-of-fit measures are also provided. Wind farms include a) Horns Rev 1 (Pedersen et al., 2023) b) Lillgrund (Pedersen et al., 2023) d) Borssele (Kainz et al., 2024) and e) Princess Amalia (Python Wind Rose). The wind rose in c) is from (King et al., 2021).

metric model will not always provide an accurate fit, but that the R^2 value should flag when this is the case. It should also be appreciated that the proposed model describes wind direction distributions only, and is independent of wind speed. Depending on context, a single Weibull wind speed distribution may be applied across all bins, separate Weibull distributions may be defined for the "prevailing" and "non-prevailing" half circles, or a different Weibull distribution may be defined for each bin.

It is hoped that the presented parametric model proves valuable to the wind industry by providing an opportunity for standardisation and enabling systematic analyses of wind direction distribution impacts and sensitivities for proposed wind farm design and control innovations.

Code and data availability. All code and data will be made freely available. A Python toolbox is being finalised, and will be made available with the final manuscript on publication.

Author contributions. EH undertook all aspects of research and paper preparation.

Competing interests. The author declares there are no competing interests.

Acknowledgements. The author would like to thank Julian Feuchtwang for originally proposing ellipse geometry as a route to wind rose modelling, and Julian Quick for stimulating discussions and assistance in tracking down wind rose data. Dr Hart is funded by a UKRI ILN+ Researcher in Residence Fellowship.

References

Amiri, A. K., Kazacoks, R., McMillan, D., Feuchtwang, J., and Leithead, W.: Farm-wide assessment of wind turbine lifetime extension using detailed tower model and actual operational history, in: Journal of Physics: Conference Series, vol. 1222, p. 012034, IOP Publishing, 2019.

160 Barrett, J. P.: The coefficient of determination—some limitations, The American Statistician, 28, 19–20, 1974.

Dallas, S., Stock, A., and Hart, E.: Control-oriented modelling of wind direction variability, Wind Energy Science Discussions, 2023, 1–42, 2023.

Hahn, G. J.: The coefficient of determination exposed, Chemtech, 3, 609–612, 1973.

Kainz, S., Quick, J., Souza de Alencar, M., Sanchez Perez Moreno, S., Dykes, K., Bay, C., Zaaijer, M. B., and Bortolotti, P.: IEA Wind
165   TCP Task 55: The IEA Wind 740-10-MW Reference Offshore Wind Plants, Tech. rep., National Renewable Energy Laboratory (NREL), Golden, CO (United States), 2024.

King, J., Fleming, P., King, R., Martínez-Tossas, L. A., Bay, C. J., Mudafort, R., and Simley, E.: Control-oriented model for secondary effects of wake steering, Wind Energy Science, 6, 701–714, 2021.

Meyers, J., Bottasso, C., Dykes, K., Fleming, P., Gebraad, P., Giebel, G., Göçmen, T., and Van Wingerden, J.-W.: Wind farm flow control:
170   prospects and challenges, Wind Energy Science Discussions, 2022, 1–56, 2022.

Pedersen, M. M., Forsting, A. M., van der Laan, P., Riva, R., Romàn, L. A. A., Risco, J. C., Friis-Møller, M., Quick, J., Christiansen, J. P. S., Rodrigues, R. V., Olsen, B. T., and Réthoré, P.-E.: PyWake 2.5.0: An open-source wind farm simulation tool, https://gitlab.windenergy. dtu.dk/TOPFARM/PyWake, 2023.

Python Wind Rose: Princess Amalia wind rose data, https://github.com/python-windrose/windrose/blob/main/samples/amalia_directionally_
175   averaged_speeds.txt, accessed: 2024-12-15.

Shu, Z. and Jesson, M.: Estimation of Weibull parameters for wind energy analysis across the UK, Journal of Renewable and Sustainable Energy, 13, 2021.

Slot, R. M. M., Schwarte, J., Svenningsen, L., Sørensen, J., and Thøgersen, M.: Directional fatigue accumulation in wind turbine steel towers, in: Journal of Physics: Conference Series, vol. 1102, p. 012017, IOP Publishing, 2018.

180 Stanley, A. P., Bay, C. J., and Fleming, P.: Enabling control co-design of the next generation of wind power plants, Wind Energy Science, 8, 1341–1350, 2023.

Yang, Z. and Dong, S.: A semi-parametric trivariate model of wind speed, wind direction, and air density for directional wind energy potential assessment, Energy Conversion and Management, 314, 118 735, 2024.

Yang, Z., Lin, Y., and Dong, S.: Joint model of wind speed and corresponding direction based on wind rose for wind energy exploitation,
185   Journal of Ocean University of China, 21, 876–892, 2022.